Bollettino di Geofisica Teorica ed Applicata Vol. 58, n. 4, pp. 377-394; December 2017
DOI 10.4430/bgta0202

Performance-based design of FRP retrofitting of existing RC frames by means of multi-objective optimisation

C. Chisari[1] and C. Bedon[2]

[1] *Department of Civil Engineering, University of Salerno, Fisciano (SA), Italy*
[2] *Department of Engineering and Architecture, University of Trieste, Trieste, Italy*

(Received: March 17, 2017; accepted: June 12, 2017)

ABSTRACT Safeguard of built heritage often involves seismic retrofitting of reinforced concrete (RC) frame structures. When strength and ductility of columns must be enhanced, an effective technique is given by the use of Fibre-Reinforced Polymer (FRP) in forms of wraps glued to the columns, which are able to improve performance thanks to confinement action. In this paper, an optimisation-based procedure for the design of FRP retrofitting of existing RC frames is described. The design aims at finding the most competitive solution in terms of cost and performance, while satisfying the damage levels imposed by Performance-Based Design for serviceability and ultimate seismic hazard levels. The resulting multi-objective optimisation problem, in which the design variables are represented by the thickness of FRP wraps, is then solved by means of Genetic Algorithms. The application to a realistic case study shows how the analysis of the resulting Pareto Front, i.e., the set of non-dominated solutions, clearly describes the threshold between cost and performance. Furthermore, interesting considerations about the sensitivity of the best solutions to the design variables can be made, improving the assessment of the optimisation results.

Key words: genetic algorithms, seismic design, pushover analysis, capacity curve.

1. Introduction and research objectives

In earthquake-prone areas, a great number of residential, commercial and public buildings is made of reinforced concrete (RC). Many of them were designed according to standards which did not take into account properly earthquake-induced effects on the structure, and thus may turn out to be particularly vulnerable. Recent catastrophic seismic events have shown that RC structures, if not correctly designed, may suffer from substantial damage in case of strong earthquakes. Thus, one of the most pressing issues in structural engineering is the assessment and the strengthening of existing heritage.

The most advanced philosophy for the analysis and design of structures, increasingly adopted by building codes, involves the concepts of performance-based capacity design (PBD) procedures. According to this approach, the engineer should proportion the building for intended nonlinear response and then use nonlinear structural analysis to verify that the structure's performance would be acceptable when subjected to various levels of ground shaking. In the case of seismic resistant concrete frames, over the last years, several authors proposed various PBD approaches, aiming

at optimising the overall performance of the given structural system (see for example SEAOC, 1995; Applied Technology Council, 1996; FEMA 356, 2000). Beck *et al*. (1998) first developed an optimisation methodology for PBD of elastic structural systems operating in an uncertain dynamic environment. Ganzerli *et al*. (2000) combined the PBD concept with structural optimisation methods, introducing a nonlinear analysis-based approach. In doing so, the performance-based constraints were defined in terms of plastic rotations of beams and columns of frames, as suggested by FEMA guidelines (FEMA 356, 2000). Zou and Chan (2005) presented a further optimisation procedure based on the "optimality criteria" concept, while Fragiadakis and Papadrakakis (2008) proposed a reliability-based optimisation approach based on nonlinear response history analysis. In accordance with this approach, an evolutionary optimisation algorithm was used to optimise RC beam and column sections in terms of cost and performance.

In the field of rehabilitation of existing buildings, among a number of other more or less common approaches (Santarsiero and Masi, 2015; Truong *et al*., 2017; Ma *et al*., 2017), the use of Fibre-Reinforced Polymers (FRP) now represents a well-established technique. Strips and grids for masonry walls and arches have been successfully applied by D'Ambrisi *et al*. (2013), Gattulli *et al*. (2014), Martinelli *et al*. (2016), while the use of FRP rebars and aggregates has been explored by Gattesco *et al*. (2015), Fava *et al*. (2016), Yazdanbakhsh *et al*. (2016). Further applications, as in the current research study, involve the use of FRP jackets for the seismic retrofitting of RC structures. When FRP jackets are used for the confinement of RC columns, in particular, the enhancement in strength and ductility of the columns can be so efficient that FRP jacketing represents one of the major retrofitting techniques for the improvement of their seismic performance. Due to this huge application of FRP jackets in practice, over the last years several researchers investigated in fact the structural behaviour of RC retrofitted elements and assemblies, see for example Balsamo *et al*. (2005), Duong *et al*. (2007), Le-Trung *et al*. (2010), Parvin *et al*. (2010), Zhu *et al*. (2011), Alaedini *et al*. (2015).

From a practical point of view, the design of FRP jackets for RC structural systems should take care of various aspects, as well as could be carried out in accordance with several existing approaches and guidelines characterized by intrinsic limitations (see for example Rocca *et al*., 2008). In this regard, optimisation techniques have proved effective in the design of such retrofitting components. Optimisation procedures have been proposed by Zou *et al*. (2007) and Choi *et al*. (2014) for the enhancement of the seismic performance of retrofitted RC frames. Zou *et al*. (2007) discussed the optimal performance-based design for FRP retrofitted RC frames. Based also on a calculation example, in particular, they showed that the seismic response of a FRP-retrofitted RC frame can be efficiently optimized when the design solution characterised by minimum thickness of the FRP jackets (hence minimum volume and material cost of the retrofitting system) satisfies interstorey-drift demand after evaluating the nonlinear structural response by means of pushover analysis. The optimisation problem was solved there by using gradient techniques after explicitly expressing the objective and the constraints in terms of design variables, i.e., FRP thickness. A Genetic Algorithm (GA) optimisation process was proposed by Chisari and Bedon (2016) for the case study examined by Zou *et al*. (2007). The advantages of GA methods for achievement of optimal FRP jacketing configurations compared to more traditional gradient methods via Taylor expansions were shown to be i) the possibility of using more complex material model descriptions accounting for softening, degradation and M-V interaction, ii) the possibility of embedding further objectives along with the minimum cost, iii) performing sensitivity analysis of the major

influencing parameters. The design of FRP retrofitting by means of optimisation techniques, and the formulation of design equations through neural networks and GAs was also explored by Cascardi *et al*. (2016), Choi (2017), Vitiello *et al*. (2017).

In this paper, the optimal design procedure is further extended to the complete design of the retrofitting system. The key novel aspect, compared to Chisari and Bedon (2016), is given by the reference design methodology, which accounts for all performance levels required for the structure in the framework of PBD. Furthermore, the methodology is characterised by the full adoption of the N2 method, unlike the preliminary procedure proposed by Chisari and Bedon (2016), where a more simplified approach was utilised.

2. FRP retrofitting of RC frame structures

FRP are composite materials made of two entities: a matrix, usually epoxy resin, and the fibres, usually glass, carbon or aramid (Kevlar). The mechanical characteristics of the two components are markedly different: whereas the matrix is isotropic with very low elastic modulus and strength (about 3 GPa and 50 MPa, respectively), the fibres can withstand loads in their axis direction only and their tensile strength and elastic modulus may reach 5000 MPa and 240 GPa, respectively (Fibre Net S.r.l., 2015). The mechanical properties of the resulting composite depend on the percentage and arrangement of the fibres with respect to the matrix.

FRP can be applied to strengthen beams, columns, and slabs of buildings and bridges. It is possible to increase the strength of structural members even after they have been severely damaged due to loading conditions. Basically, FRP (and Carbon FRP in particular, CFRP) is available in different geometries: precured laminates (rods or plates) manufactured by pultrusion; wet lay-up systems (uni- or bidirectional fabrics) in which resin is used as matrix and adhesive; prepreg systems, i.e., reinforcement fibres or fabrics into which a pre-catalysed resin system has been impregnated by a machine. In this work, the focus will be on wet lay-up wraps used to strengthen RC columns.

When FRP wraps are glued to RC columns placing them with the fibre direction orthogonal to primary axis of the members, they produce a confinement action which opposes the expansion of the concrete core, thus causing a state of triaxial stress inside the element (Realfonzo and Napoli,

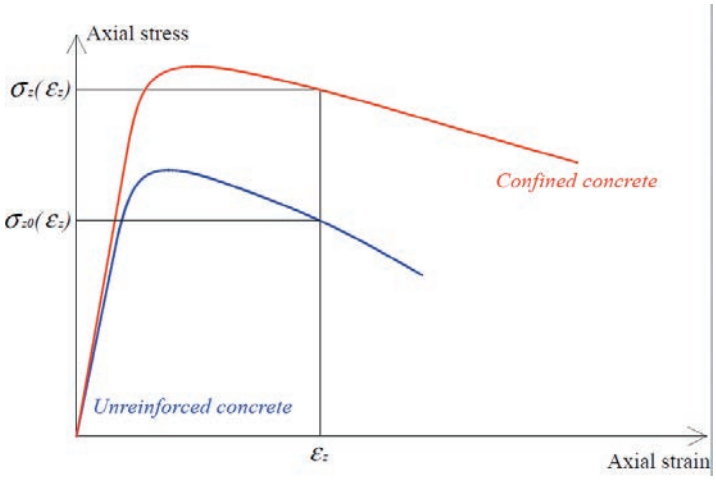

Fig. 1 - Change in the stress-strain relationship for concrete as effect of confinement.

2013; Realfonzo *et al*., 2013). This can be macroscopically accounted for as a change in the stress-strain relationship, with an increase in concrete strength and ductility (Fig. 1).

Many authors have proposed mathematical material models for concrete in which the constitutive relationship is modified as an effect of the confinement action of the FRP wraps (Samaan *et al*., 1998; Lam and Teng, 2009; Megalooikonomou *et al*., 2012). In general, such models should consider the confinement effect exerted by both transversal reinforcement and FRP wraps, with deterioration phenomena if relevant (dynamic analyses). An example of such model, used in the applicative example described in Section 4, is represented by the model developed by Braga *et al*. (2006) and implemented in Opensees software package (OpenSees, 2010) by D'Amato *et al*. (2012). In the referenced works, the model has proved to simulate accurately the behaviour of confined concrete on a large database of experimental cases. Starting from the unconfined stress-strain relationship $\sigma_{z0}(\varepsilon_z)$, the stress of confined concrete is obtained by adding the quantity:

$$\Delta\sigma_z(\varepsilon_z) = 2\,\nu\,B\,l^2 \tag{1}$$

where ν is Poisson's ratio, l is the semi-length of the core section and B is the Airy's constant, which was evaluated by Braga *et al*. (2006) as a function of FRP mechanical and geometrical characteristics.

3. Performance-based design (PBD) approach and multi-objective optimisation

3.1. General PBD concepts

PBD for seismic resistant structures (PBSD) represent a well-established process for the seismic analysis of buildings (including new buildings as well as retrofitting of existing structural systems), being characterized by the specific intent to achieve defined performance objectives in future earthquakes. Performance objectives for a given structure are strictly related to expectations regarding the amount of damage the building may experience in response to earthquake shaking, and the consequences of that damage.

The reference performance objectives are detected as Operational (O), Immediate Occupancy (IO), Life Safety (LS), Collapse Prevention (CP). These performance objectives are reached when the corresponding levels of overall damage are not overcome when the structure undergoes earthquake ground motion characterised by decreasing probability of exceedance during its nominal life time. Clearly, this approach entails the definition of a Damage Measure (DM) and an Earthquake Hazard Level (HL). An indicative and meaningful DM suggested by standard codes is the interstorey drift ratio, i.e., the ratio between the relative displacement between upper and lower floor at given level of the structure (displacement - based design: DBD) and the interstorey height. The HL is usually described by Peak Ground Motion of the earthquake, or globally by the design spectrum corresponding to the given probability of exceedance. As such, given a structural typology, the performance levels are verified by comparing the demand at given HL with specific limit displacement values and reference interstorey drift amplitudes. Basically, the overall design process follows the approach given in Fig. 2.

In this research study, the PBD method is considered in conjunction with a GA optimisation approach for the seismic retrofitting of RC frames with FRP jackets.

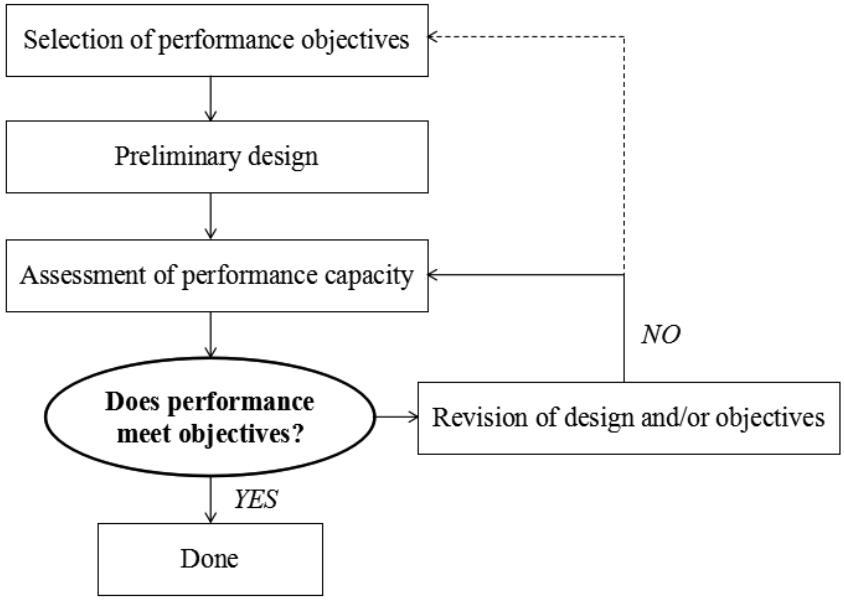

Fig. 2 - General flow chart for PBD process.

3.2. Displacement-based approach to inelastic structures

The DBD approach proposed by Fajfar and Gašperšič (1996), called N2 method, develops into two fundamental phases. Firstly, the capacity curve of the structure, describing the evolution of the structural response with increasing seismic intensity, must be determined. This is obtained through a pushover analysis, in which static lateral forces on the structure are proportionally increased until collapse. The second stage consists of identifying the performance point (PP) corresponding to the nonlinear response of the frame due to the assigned earthquake. This entails the study of elastic-plastic single-degree-of-freedom (SDOF) system equivalent to the real structure modelled as multi-degree-of-freedom (MDOF) system. After establishing the PP in terms of SDOF displacement, the corresponding control displacement of the structure is evaluated and all quantities of interest extracted from the capacity curve. In the case of DBD, interstorey drifts at PP are checked against the performance level requirements.

3.2.1. Evaluation of the capacity curve

The capacity curve represents the relationship between base shear and top displacement of the structure, when a system of lateral forces is applied to the structure and increased proportionally until collapse. The main ingredients of this step are: i) the structural model, ii) the force distribution, and iii) the definition of collapse. The structural model must represent the real behaviour with a sufficient degree of accuracy, and should account for all sources of nonlinearities occurring in the structure. A suitable approach, used in this work, consists of modelling structural members as nonlinear beams having fibre section, and using a material model for concrete as that proposed by Braga *et al*. (2006) and D'Amato *et al*. (2012). The force distribution is determined by multiplying the mass matrix by an acceleration profile. According to Italian building standard NTC2008 (Decreto Ministeriale 14 Gennaio 2008, 2008), two acceleration profiles should be used: the first

one is coincident to the first mode shape, while the second one is constant. The collapse is defined as the point corresponding to a reduction in global strength, i.e., base shear, up to 85% of the maximum structural capacity.

3.2.2. Equivalent bilinear SDOF

The application of the N2 method requires the use of an equivalent elastic-plastic SDOF to represent the global behaviour. Force F^* and displacement d^* of the equivalent system are related to the corresponding quantities F_b and d_c, base shear and top displacement of the real system, respectively, by the relationships:

$$F^* = \frac{F_b}{\Gamma}$$
$$d^* = \frac{d_c}{\Gamma} \tag{2}$$

where Γ is the modal participation factor, defined as:

$$\Gamma = \frac{\boldsymbol{\varphi}^T \boldsymbol{M} \boldsymbol{\tau}}{\boldsymbol{\varphi}^T \boldsymbol{M} \boldsymbol{\varphi}} \tag{3}$$

In Eq. 3, $\boldsymbol{\tau}$ is the influence vector, $\boldsymbol{M}$ the mass matrix and $\boldsymbol{\varphi}$ the first modal shape vector, normalised such that $d_c = 1$. The mass of the equivalent SDOF is defined as $m^* = \boldsymbol{\varphi}^{\mathrm{T}} \boldsymbol{M} \boldsymbol{\tau}$. After this change of variables, the capacity curve must be converted into a bilinear system, having stiffness k^* equal to the secant stiffness at 0.6 $F_{bu}{}^*$, while the yielding force is evaluating by equating the areas under the capacity curve and the bilinear curve respectively. This implies:

$$F_y^* = k^* d_u^* \left(1 - \sqrt{1 - \frac{2E_b}{k^* \, {d_u^*}^2}} \right) \tag{4}$$

where d_u^* is the ultimate displacement of the system and E_b is the area under the capacity curve.

3.2.3. Identification of the Performance Point

The displacement demand of the nonlinear system depends on the elastic period T^* of the equivalent SDOF. If $T^* \geq T_C$, corresponding to the limit between the constant pseudo-acceleration and constant pseudo-velocity, the inelastic demand d^*_{max} is equal to that of an elastic system with same period $d^*_{e,max}$; otherwise it may be evaluated as:

$$d^*_{max} = \frac{d^*_{e,max}}{q^*} \left[1 + (q^* - 1) \frac{T_C}{T^*} \right] \geq d^*_{e,max} \tag{5}$$

where $q^* = S_e(T^*) \frac{m^*}{F_y^*}$, with $S_e(T^*)$ ordinate of the elastic design spectrum at T^*, represents the ratio between elastic response force and yielding force of the equivalent system. If $q^* \leq 1$, it is assumed that $d^*_{max} = d^*_{e,max}$.

3.2.4. Displacement checks

The primary check consists of verifying that the ductility demand of the system is lower than the capacity. This correspond to the inequality $d^*_{max} \leq d^*_u$, the satisfaction of which may be critical at LS and CP performance levels. Once this has been verified, the verification of the damage state of the structure may be carried out by evaluating the interstorey drifts corresponding to the PP top displacement $d^*_{c,max} = \Gamma d^*_{max}$ and comparing them to the limits prescribed by the code.

3.2.5. Computational cost

The complete verification procedure for the design of a new building or a retrofitting action requires that more than one force distribution and more than one earthquake hazard level [and, consequently, performance points (PPs) and checks] should be considered. Whereas the capacity curve is the result of a nonlinear FE analysis, and thus the introduction of a further force distribution doubles the analysis time, the computational time required by steps described in sections 3.2.2 to 3.2.4 is usually negligible compared with that for step in section 3.2.1 and so multiple earthquake intensity levels may be readily considered without excessive computational effort.

3.3. Optimal PBD design

The procedure described in the previous sub-section represents a general verification procedure, which, applied to FRP retrofitting of RC frames, gives as output a simple "yes/no" answer to the question "Does the retrofitted structure satisfy the performance requirements for the given earthquake hazard levels?". However, a far more effective procedure may be developed in the framework of structural optimisation. The designer, implicitly or explicitly, always searches for a structure characterised by minimal cost. Hence, the most rigorous and effective method to achieve this goal consists of formulating the design as an optimisation problem in which the performance checks act as constraints, while the cost is the objective to minimise. Generally, the cost is assumed proportional to the weight of the structure, possibly scaling differently components made of different materials. In some cases, costs not directly dependent on the weight (i.e., due to transportation, welding, etc.) may be embedded in the procedure through specific terms in the cost function. Objectives and constraints depend on some input variables $\boldsymbol{x}$ which are varied in the search for the solution. The space of the values that can be assumed by the input variables is called 'design space'. Further enhancements may be accomplished if, more realistically, a larger number of objectives are considered (Chisari and Bedon, 2016). If they refer to performance objectives, as in this work, where the ductility supply provided by the retrofitting system is maximised, a deep investigation on the threshold between cost and performance may be accomplished.

Once the design space, the objective and the constraints are set, the solution of an optimisation problem may be obtained by using different approaches. Basically, the cheapest methods in terms of computational burden (i.e., number of evaluations of the objective function) are those based on the evaluation of the gradient of the objective function [steepest descend: Box *et al*. (1969); trust region: Byrd *et al*. (1987)]. When the objective function is not explicitly known (as in the present case, where it results from the evaluation of FE model) and no information about the convexity of the function is present and, even more, in case of multi-objective optimisation, less efficient but more general methods are preferred. Among those, GAs (Goldberg, 1989) are rather popular because of their ability to solve different typologies of problems (Chisari *et al*., 2015, 2016, 2017) and will be used in this work. Unlike gradient-based methods, GAs improve a set of possible

solutions (called population) in average according to the predefined constraints and objectives.

The general scheme which must be followed when PBD of FRP retrofitting systems is approached by a GA optimisation procedure is outlined in Fig. 3. After defining a template FE model and setting up the GA parameters, the analysis consists of evaluating the trial solutions of each population, i.e., running the FE model (one or more if several force distributions are used), extracting output variables (i.e., interstorey drift, internal forces, displacements) at PP corresponding to different HLs and evaluating objectives and constraints.

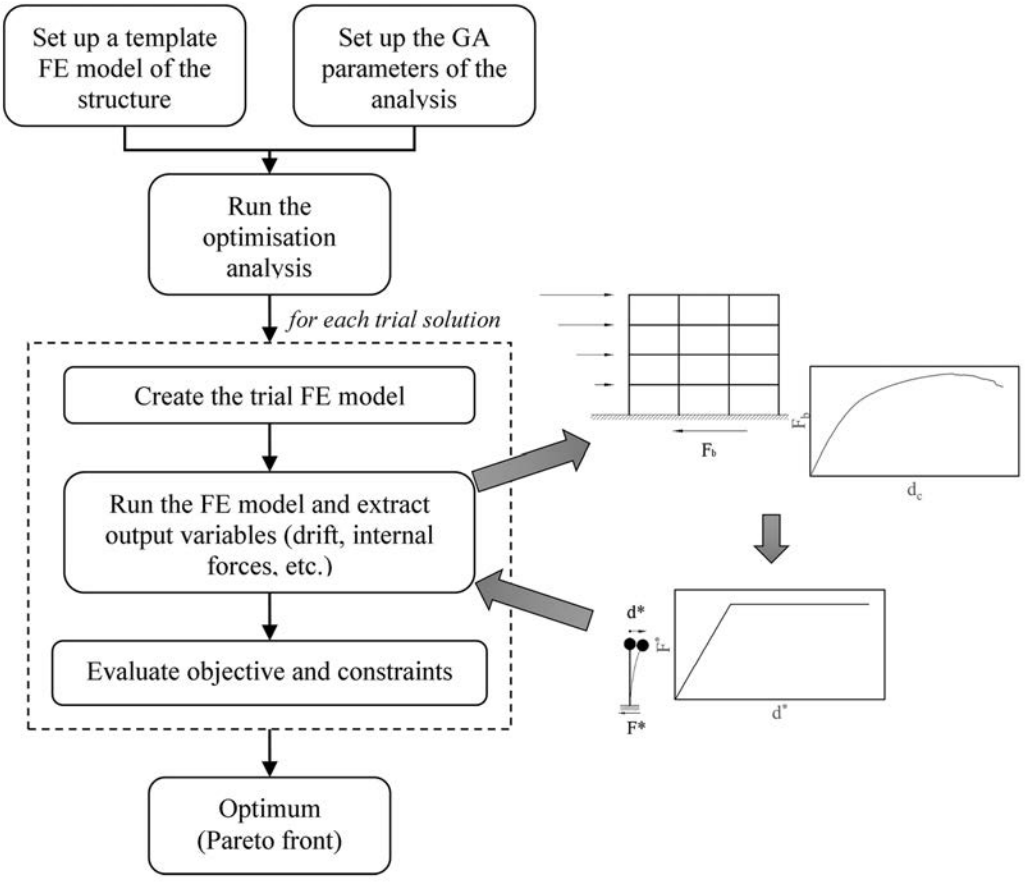

Fig. 3 - Flow chart of the optimisation process.

4. Case study

As a reference case study, the 4-storey, 3-bay RC frame displayed in Fig. 4 was investigated. A 350×550 mm cross-section was considered for all the beams. The internal and external columns were 500 mm- and 350 mm-dimension square columns, respectively. The details of the reinforcement for the RC frame elements are shown in Fig. 4a.

The reference frame is considered as part of an office building, with 50-year nominal life, supposed to be located in Catania (Italy). The example has been selected as a typical building designed according to modern codes but without consideration of the seismic action, since Catania

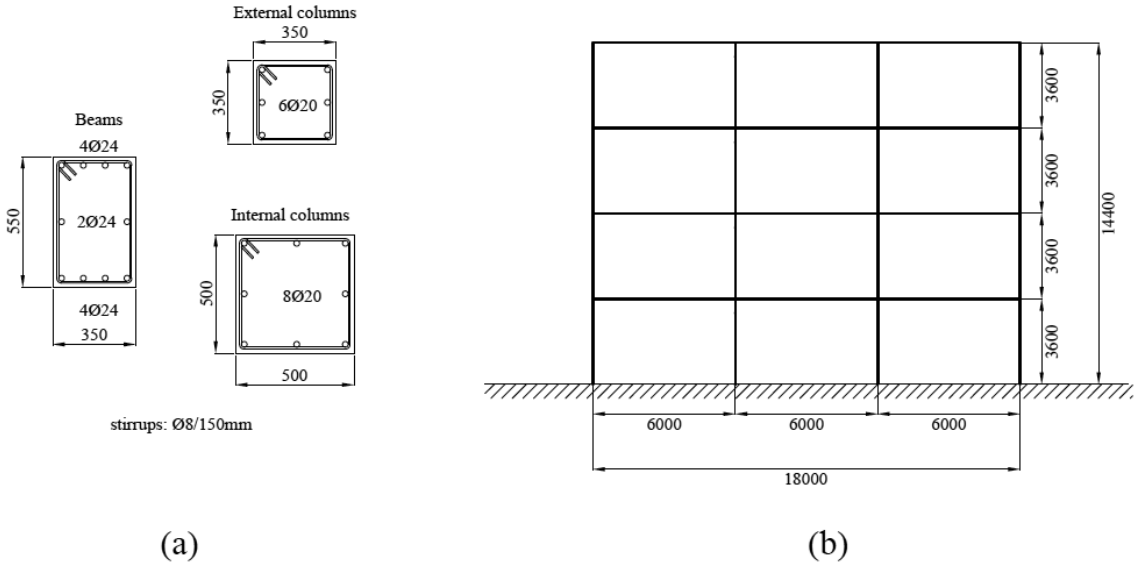

Fig. 4 - a) Cross-section properties for the concrete structural elements, and b) front view of the structure. Nominal dimensions in millimetres.

area has not been considered as seismically relevant until recent years (1981). For this reason, it will be seen that the bare frame does not comply with code prescriptions about interstorey drift ratio. According to Italian Seismic Code NTC2008, the structure is considered as Use Class II, and the reference parameters for seismic action modelling (exceedance probability and seismic risk parameters) are displayed in Table 1. Considering Subsoil Category 2, Topographic Category T1 and damping ratio 5%, the corresponding elastic design spectra for the 4 performance levels are shown in Fig. 5.

Table 1 - Reference seismic action parameters.

Performance level	Exceedance probability during Nominal Life	Return Period [year]	a_g [g]	F_0 [-]	T_C^* [s]
Operational	81%	30	0.0623	2.55	0.242
Immediate Occupancy	63%	50	0.0766	2.55	0.264
Life Safety	10%	475	0.2063	2.46	0.358
Collapse Prevention	5%	975	0.2834	2.42	0.443

In terms of mechanical calibration of materials, concrete was assumed to have an unconfined compressive strength of f_c = 21 MPa. According to the formulation proposed by the Model Code (International Federation for Structural Concrete, 2012), the corresponding Young modulus was set equal to E_c = 30,660 MPa, while the ultimate strain for confined concrete was assumed as ε_2 = 0.00356. The steel reinforcement was then characterized by Young modulus E_s = 210 GPa, yielding stress f_y = 300 MPa, strain-hardening ratio 0.01 and ultimate strain equal to 3%. Finally, the FRP reinforcement was considered in the form of an elastic-brittle material, with Young modulus E_f = 230 GPa and ultimate strain $\varepsilon_{f,u}$ = 0.00913, corresponding to an ultimate stress $\sigma_{f,u}$ = 2100 MPa. This latter value represents the FRP hoop strength, significantly lower than the flat coupon strength obtained in tensile tests.

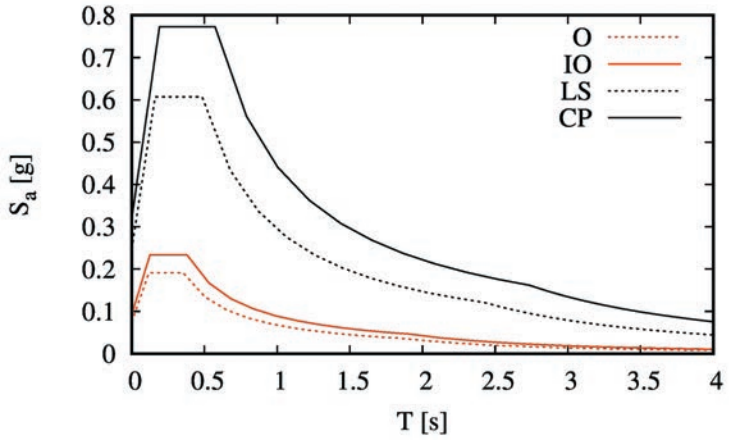

Fig. 5 - Elastic design spectra for the case study.

The RC frame was modelled in OpenSees. All the frame members were represented by nonlinear force-based elements, in which the constitutive law at element level is evaluated by the fibre-approach applied to the cross-section. In particular, forceBeamColumn element type was used, which is based on the non-iterative (or iterative) flexibility formulation. The locations and weights of the element integration points are based on so-called plastic hinge integration, which allows the user to specify plastic hinge lengths at the element ends (Scott and Fenves, 2006). Two-point Gauss integration is used on the element interior while two-point Gauss-Radau integration is applied over lengths of $4L_p$ and $4L_p$ at the element ends, where L_p is the plastic hinge length, assumed here as $L_p = 0.08L + 0.022 f_y d_b$ in which L is the member length and d_b is the longitudinal reinforcing bar diameter (Paulay and Priestley, 1992).

The material model utilized for the confined concrete is the ConfinedConcrete01 characterized by the capability to estimate the increment of strength and ductility due to the FRP confinement. The model needs not to be changed in case of absence of FRP jacket. The material model for the steel reinforcement was the Giuffrè-Menegotto-Pinto model. It must be emphasized that, although accurate enough to capture beam and column failure, the model cannot predict non-ductile joint panel failure, which can be relevant in case of existing buildings. More advanced modelling approaches should be used to this aim (De Risi *et al*., 2017). Furthermore, the presence of infill panels can affect the overall response (Chaker and Cherifati, 1999; Al-Chaar *et al*., 2002) and should be properly modelled in real cases. Given the illustrative purpose of this worked example and the high variability of the infill panel response (which depends on the characteristics of its components, their arrangement, the presence of openings and the bond condition with the RC frame), the effect of infill panels on the structure was neglected at this stage.

The columns were fixed at the base. A first loading step accounting for gravity load was considered, before performing the pushover analyses. The gravity loads consisted of the self-weight $\gamma = 23000$ N/m^3 plus a distributed load equal to $p = 50$ kN/m on the beams. Afterwards, two load distributions for pushover analyses were considered separately, the first (D1) with horizontal loads increasing proportionally to $\boldsymbol{M\varphi}$ where $\boldsymbol{M}$ is the mass matrix and $\boldsymbol{\varphi}$ the first-mode shape, and the second (D2) with horizontal loads proportional to the seismic masses. P-Δ effects were not taken into account.

The total mass of the RC frame, considering the seismic masses corresponding to the aforementioned loads, was estimated to be equal to 392.12 t.

4.1. Analysis of the bare frame

A preliminary modal analysis was performed on the bare frame; the periods of the first three modes are displayed in Table 2, along their modal masses. As the first mode has a participating mass equal $m = 84.49\% > 75\%$, the use of force distribution D1 is allowed by NTC2008. The first-mode shape, normalised with respect to the mass, is represented in Fig. 6 with an amplification factor equal to 4000.

Table 2 - Results of the modal analysis of the bare frame.

Mode of vibration	Period [s]	Participating mass
1	0.796	84.49%
2	0.256	10.25%
3	0.148	3.48%

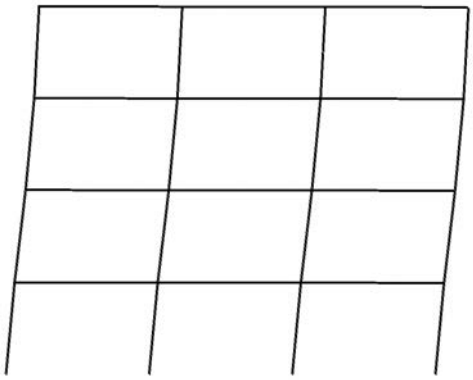

Fig. 6 - First-mode shape of the bare frame.

The results of the pushover analysis, as described in Section 6 for the bare frame, are reported in Table 3. It is evident that the limits proposed by NTC2008 for serviceability limit states (0.5% at IO for rigid partitions interfering with the structure flexibility; 2/3 of the previous for Operational Performance Level) are verified for both force distributions; on the contrary, the top floor demand required by LS and CP levels by FEMA 356 (2000) (which is applied as NTC2008 does not provide limits for ultimate limit states) are not met by the structural capacity. The capacity curve is displayed in Fig. 7, from which it is possible to deduce minimum ductility $\mu = \min(\mu^{D1}, \mu^{D2}) = 3.54$, corresponding to a behaviour factor $q = 2.28$.

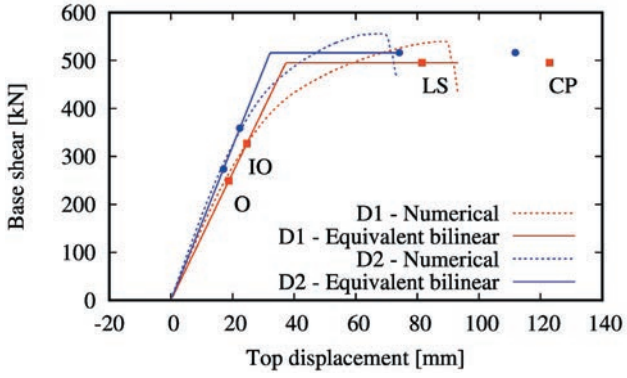

Fig. 7 - Capacity curves for the bare frame.

Table 3 - Results of the pushover analysis on the bare frame.

Force distribution	Performance level	Maximum interstorey drift ratio	Interstorey drift ratio limit	Top floor demand [mm]	Top floor capacity [mm]
D1	O	0.206%	0.333%	18.78	93.20
	IO	0.269%	0.500%	24.61	93.20
	LS	0.911%	1.000%	81.50	93.20
	CP	-	4.000%	122.89	93.20
D2	O	0.185%	0.333%	17.07	73.57
	IO	0.239%	0.500%	22.39	73.57
	LS	-	1.000%	74.14	73.57
	CP	-	4.000%	111.79	73.57

4.2. Optimal design of the FRP reinforcement

The problem of properly designing the FRP retrofitting system for a RC frame can be stated as:

$$
\begin{aligned}
&\text{Find} && \tilde{\boldsymbol{t}} = [t_{1,1}, \dots, t_{1,4}, t_{2,1} \dots, t_{2,4}, t_{3,1} \dots, t_{3,4}, t_{4,1} \dots, t_{4,4}] \\
&\text{Minimizes} && w(\boldsymbol{t}) \\
& && -\mu(\boldsymbol{t}) = -\min\left(\mu^{D1}(\boldsymbol{t}), \mu^{D2}(\boldsymbol{t})\right) \\
&\text{Subjected to} && \\
& \text{(a)} && \max\left(u^{D1}_{demand,\mathrm{IO}}\ (\boldsymbol{t})/u^{D1}_{y}(\boldsymbol{t}), u^{D2}_{demand,\mathrm{IO}}\ (\boldsymbol{t})/u^{D2}_{y}(\boldsymbol{t})\right) \le 1 \\
& \text{(b)} && \max\left(u^{D1}_{demand,\mathrm{CP}}\ (\boldsymbol{t})/u^{D1}_{u}(\boldsymbol{t}), u^{D2}_{demand,\mathrm{CP}}\ (\boldsymbol{t})/u^{D2}_{u}(\boldsymbol{t})\right) \le 1 \\
& \text{(c)} && \max\left(d^{Dj}_{i,O}\ (\boldsymbol{t})\right) \le 0.333\%\ \ i{=}1,\dots,4;\ j{=}1,2 \\
& \text{(d)} && \max\left(d^{Dj}_{i,\mathrm{IO}}\ (\boldsymbol{t})\right) \le 0.5\%\ \ i{=}1,\dots,4;\ j{=}1,2 \\
& \text{(e)} && \max\left(d^{Dj}_{i,LS}\ (\boldsymbol{t})\right) \le 1\%\ \ i{=}1,\dots,4;\ j{=}1,2 \\
& \text{(f)} && \max\left(d^{Dj}_{i,\mathrm{CP}}\ (\boldsymbol{t})\right) \le 4\%\ \ i{=}1,\dots,4;\ j{=}1,2
\end{aligned}
\qquad (6)
$$

where

- $t_{h,k}$ is the FRP wrap thickness at column h and storey k;
- $w(\boldsymbol{t})$ is the total volume of the FRP reinforcement;
- $\mu = u_u/u_y$ is the ductility, with u_y, u_u are the top displacement at yielding and ultimate state respectively;
- d_i^{Dj} is the interstorey drift ratio at floor i for force distribution D_j.

By imposing the double objective, i.e., minimisation of the FRP volume and maximisation of ductility, it is possible to highlight the threshold between cost and performance. The optimisation analyses were then conducted according the scheme described in the previous sections. A GA with the following properties was used:

- initial population creation: Sobol sequence;
- population size: 50 individuals;
- number of generations: 50;

- ranking type: linear, with scaling pressure 2.0;
- selection type: stochastic universal sampling;
- crossover type: BLX-α, with probability 1.0 and parameter α=2.0;
- mutation type: aleatory, with probability 0.007;
- NSGA-II approach (Deb *et al.*, 2002), in which ranking is based sequentially on: i) constraint satisfaction, ii) domination, and iii) crowding distance was adopted to solve the multi-objective optimisation. The GA was implemented in the software TOSCA (Chisari, 2015).

As design variable for the optimisation problem, the thickness of the FRP wraps applied to the columns was considered. In particular, different thicknesses were assumed for external and internal columns and for each floor. The problem consisted thus of eight design variables (four floors times two column typologies). The FRP thicknesses were allowed to vary between 0 (no reinforcement) to 2 mm, with 0.001 mm increments.

In Fig. 8 the scatter plots of the solutions analysed during the optimisation analysis in terms of FRP volume vs. interstorey drift checks are displayed. It is evident that all solutions satisfy serviceability limit states, and the effect of the reinforcement is negligible. This is expected, since the bare frame is characterised by interstorey drifts already below the elastic limit, and the effect of FRP reinforcement in this behavioural range is null, i.e., it acts on strength and ductility, but not on stiffness of the structural system. On the contrary, the effect on ultimate limit states is more pronounced, but only LS condition requires retrofitting to be satisfied, while all solutions are well below CP limit. However, this plots do not consider solutions not satisfying constraints (a) or (b) in Eq. 6. This becomes clearer if one looks at Fig. 9, where those conditions are plotted against FRP volume. It is evident that condition (a) is always satisfied, meaning that even without reinforcement the demand at IO is below the elastic limit of the equivalent bilinear system. On the contrary, the ultimate top displacement demand at CP may not be attained if the retrofitting system is not well-designed. The need of increasing ductility to achieve demand was already noticed

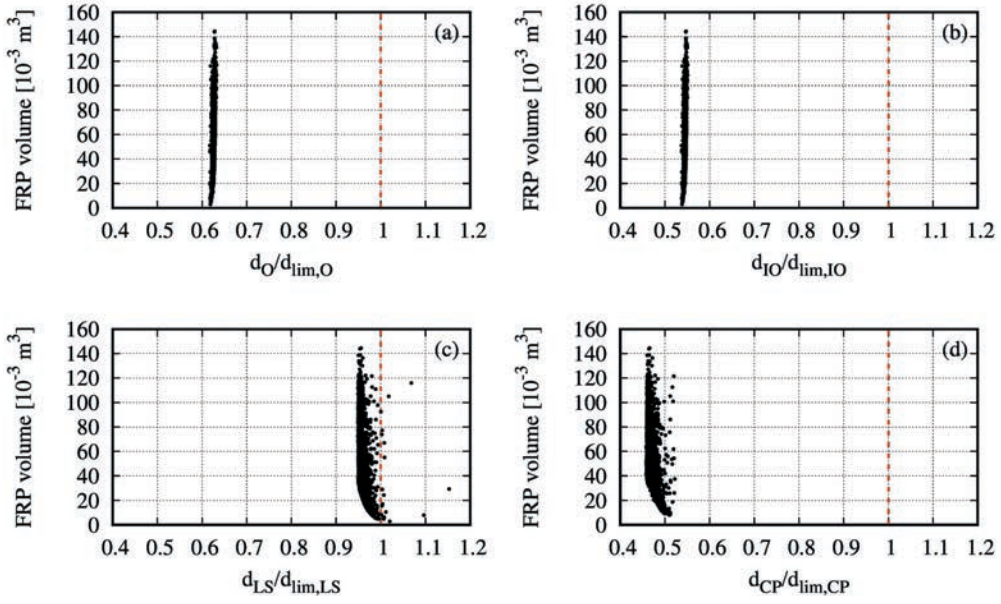

Fig. 8 - Scatter plots of the solutions analysed during the optimisation analysis in terms of FRP volume vs. interstorey drift check at: a) O, b) IO, c) LS, d) CP levels.

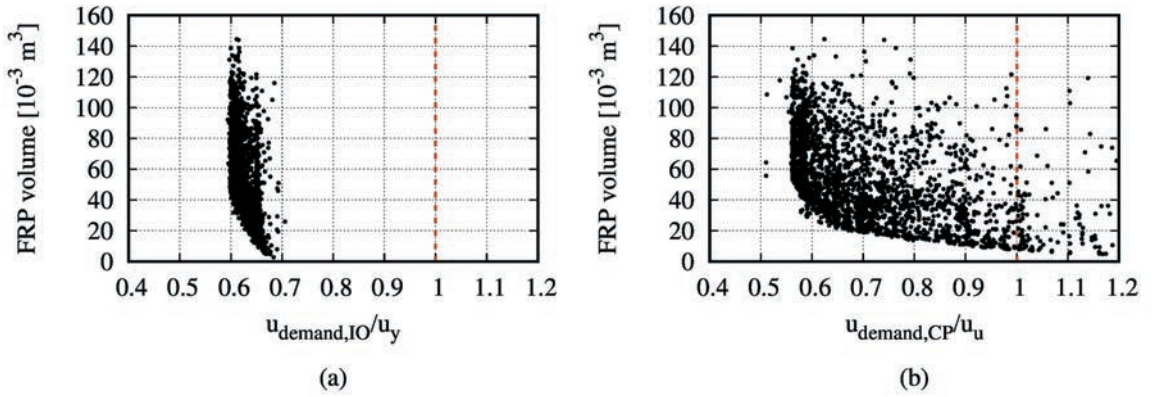

Fig. 9 - Scatter plots of the solutions analysed during the optimisation analysis in terms of FRP volume vs. displacement check at: a) IO, b) CP.

from the results of the bare frame displayed in Table 3; however, it is interesting to note that even large values of FRP reinforcement may not lead to the satisfaction of ductility demand (existence of points in the top-right part of Fig. 9b).

The Pareto Front, i.e., the set of non-dominated solutions in the objective space, is displayed in Fig. 10. We can identify three regions in the plot. In the region bound by a red rectangle, it is possible to notice an approximately linear trend between ductility and FRP volume from the minimum value μ=5.23 until approximately μ=8.41. After this value (blue rectangle), a small increase in ductility can only be achieved at expenses of a large increment of cost (almost vertical branch). In the last two design points (inside the green rectangle), compared to the previous area, a small increment in FRP volume causes a significant increase in ductility. From these observations, it seems reasonable to suppose that the points belonging to the blue area are anomalous in the context of the Pareto Front, and probably related to a non-optimal path of the analysis. In the following, thus, we will be concerned about the design points identified by the red rectangle, i.e., the area where FRP volume and ductility are characterized by a quasi-linear trend.

One of the advantages of the optimisation approach proposed here is the possibility of studying the sensitivity of the best solutions to the input variables. While it is obvious that FRP volume is linearly correlated to the thickness, since the width and length of the wraps are constant, the dependence of ductility on FRP reinforcement for the Pareto Front individuals may be highlighted

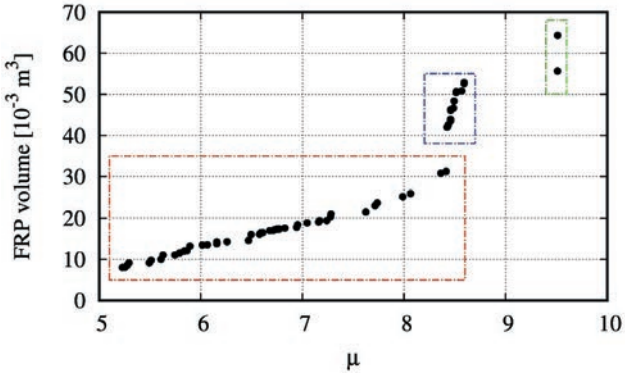

Fig. 10 - Pareto front of the optimisation analysis.

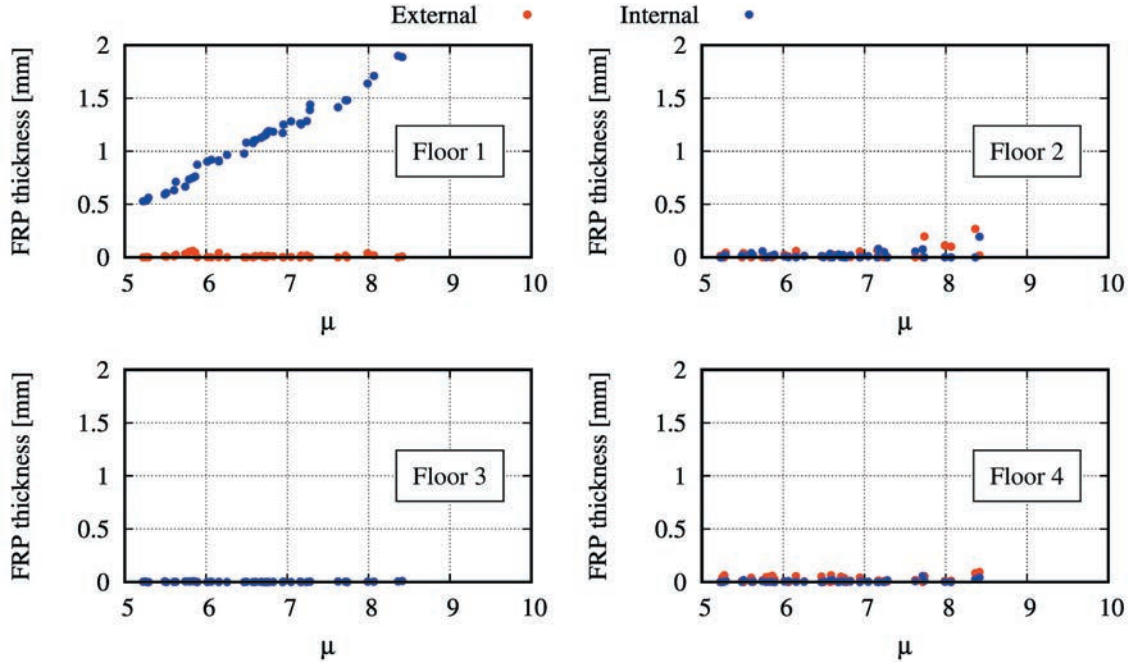

Fig. 11 - Dependence of ductility on FRP wrap thickness, as obtained for internal/external columns at each floor.

in scatter plots as those displayed in Fig. 11. It is evident here that the only design variable responsible of increasing ductility is the FRP thickness at floor 1 for the internal columns, which is almost linearly related to μ. To keep FRP volume as low as possible, all the other FRP reinforcement is selected to be close to zero.

Finally, in Fig. 12 the capacity curve of the best solutions according the two objectives (cost and ductility) are shown. It is evident that to minimize cost the most stringent constraint (CP top displacement demand for D2 force distribution) is attained without safety margins, i.e., the demand

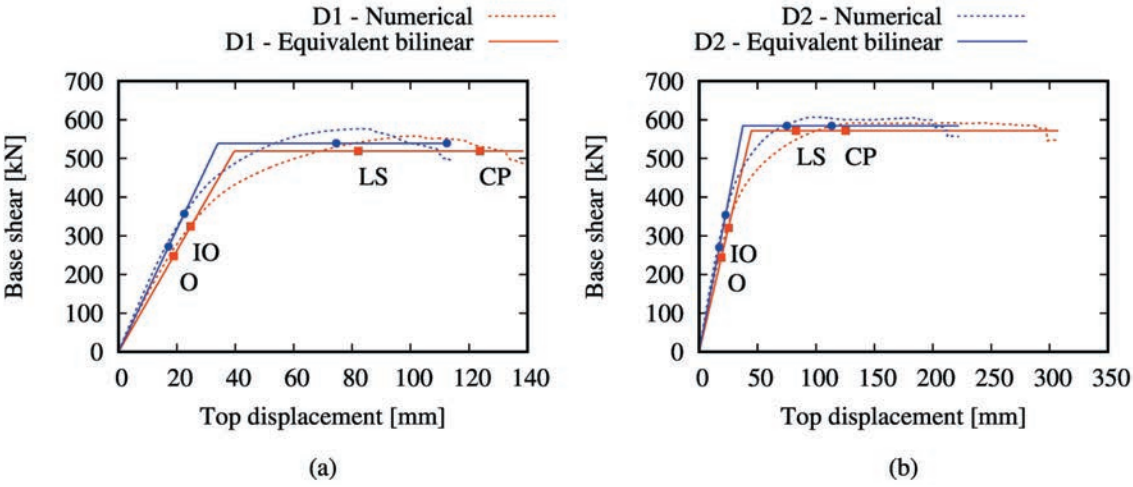

Fig. 12 - Retrofitted frame capacity curves: a) best cost solution, and b) best ductility solution.

is coincident with the end of the capacity curve. On the contrary the best solution according to ductility objective presents larger safety margin against collapse.

5. Summary and conclusions

In this work, the optimal PBD of a retrofitting system made of FRP wraps for RC frame structures is proposed. The design is formulated as an optimisation problem in which the cost of the system is minimised and the overall ductility of the structure maximised, with the constraints given by building code about interstorey drifts at different levels of seismic intensity. The problem is then solved by means of GA.

A case study is considered, in which seismic retrofitting of an existing RC frame not satisfying code prescriptions must be designed by means of the proposed technique. The results show that feasible solutions may be readily found, and the threshold between cost and performance is investigated by studying the Pareto Front of the multi-objective optimisation. In the specific case, it is possible to apply retrofitting on the internal columns at first floor only, while FRP wraps are mostly ineffective at the other floors and at the external columns. The minimum-cost solution is located at the boundary between the feasible and unfeasible region of the solution space, i.e., it strictly satisfies the performance constraints without providing adequate safety margins. These could be directly inserted in the constraint formulation or another solution belonging to the Pareto Front but characterized by larger ductility may be selected.

The proposed procedure has the desirable property to be general and applicable to any kind of structure, provided that an appropriate modelling of the basic seismic behaviour is carried out. For this reason, further developments will focus on more accurate modelling of the structures (by including joint failure and infill panel contribution) and the effect of different material models for confined concrete on the optimal solution provided by the procedure. This preliminary study will also serve to set up a parametric study aimed at providing general recommendations for the design of FRP retrofitting.

Acknowledgements. The study described in this paper derives from the research investigations originally presented at the National GNGTS 2016 Congress in Lecce (Italy). In this regard, the Italian AGLC association is gratefully acknowledged for financially supporting part of the activities (research award for early stage researchers).

REFERENCES

Al-Chaar G., Issa M. and Sweeney S.; 2002: *Behavior of masonry-infilled nonductile reinforced concrete frames*. J. Struct. Eng., **128**, 1055-1063.

Alaedini S., Kabir M. and Hejabi H.; 2015: *Seismic ductility evaluation of shear-deficient RC frames strengthened by externally bonded CFRP sheets*. KSCE J. Civil Eng., **20**, 1925-1935.

Applied Technology Council; 1996: *(ATC-40) seismic evaluation and retrofit of concrete buildings, volume 1*. Report No. SSC 96-01, Redwood City, CA, USA, 346 pp.

Balsamo A., Colombo A., Manfredi G., Negro P. and Prota A.; 2005: *Seismic behavior of a full-scale RC frame repaired using CFRP laminates*. Eng. Struct., **27**, 769-780.

Beck J., Papadimitriou C., Chan E. and Irfanoglu A.; 1998: *A performance-based optimal structural design methodology*. Report No. EERL 97-03, California Institute of Technology, Pasadena, CA, USA, 45 pp.

Box M.J., Davies D. and Swann W.H.; 1969: *Non-linear optimization techniques*. In: Oliver and Boyd (eds), Imperial Chemical Industries Monograph, Edinburgh, United Kingdom, 68 pp.

Braga F., Gigliotti R. and Laterza M.; 2006: *Analytical stress-strain relationship for concrete confined by steel stirrups and/or FRP jackets*. J. Struct. Eng., **132**, 1402-1416.

Byrd R.H., Schnabel R.B. and Shultz G.A.; 1987: *A trust region algorithm for nonlinearly constrained optimization*. SIAM J. Numer. Anal., **24**, 1152-1170.

Cascardi A., Micelli F. and Aiello M.; 2016: *Analytical model based on artificial neural network for masonry shear walls strengthened with FRM systems*. Composites Part B, **95**, 252-263.

Chaker A. and Cherifati A.; 1999: *Influence of masonry infill panels on the vibration and stiffness characteristics of R/C frame buildings*. Earthquake Eng. Struct. Dyn., **28**, 1061-1065.

Chisari C.; 2015: *Inverse techniques for model identification of masonry structures*. Ph.D. Thesis in Scienze dell'Ingegneria, University of Trieste, Trieste, Italy, 277 pp.

Chisari C. and Bedon C.; 2016: *Multi-objective optimization of FRP jackets for improving seismic response of reinforced concrete frames*. Am. J. Eng. Appl. Sci., **9**, 669-679.

Chisari C., Bedon C. and Amadio C.; 2015: *Dynamic and static identification of base-isolated bridges using genetic algorithms*. Eng. Struct., **102**, 80-92.

Chisari C., Macorini L., Amadio C. and Izzuddin B.A.; 2016: *Optimal sensor placement for structural parameter identification*. Struct. Multi. Optim., **55**, 647-662, doi:10.1007/s00158-016-1531-1.

Chisari C., Francavilla A.B., Latour M., Piluso V., Rizzano G. and Amadio C.; 2017: *Critical issues in parameter calibration of cyclic models for steel members*. Eng. Struct., **132**, 123-138.

Choi S.; 2017: *Investigation on the seismic retrofit positions of FRP jackets for RC frames using multi-objective optimization*. Composites Part B, **123**, 34-44.

Choi S., Kim Y. and Park H.; 2014: *Multi-objective seismic retrofit method for using FRP jackets in shear-critical reinforced concrete frames*. Composites Part B, **56**, 207-216.

D'Amato M., Braga F., Gigliotti R., Kunnath S. and Laterza M.; 2012: *A numerical general-purpose confinement model for non-linear analysis of R/C members*. Comput. Struct., **102-103**, 64-75.

D'Ambrisi A., Feo L. and Focacci F.; 2013: *Experimental and analytical investigation on bond between Carbon-FRCM materials and masonry*. Composites Part B, **46**, 15-20.

De Risi M., Ricci P. and Verderame G.; 2017: *Modelling exterior unreinforced beam-column joints in seismic analysis of non-ductile RC frames*. Earthquake Eng. Struct. Dyn., **46**, 899-923.

Deb K., Pratap A., Agarwal S. and Meyarivan T.; 2002: *A fast and elitist multiobjective genetic algorithm: NSGA-II*. IEEE Trans. Evol. Comput., **6**, 182-197.

Decreto Ministeriale 14 Gennaio 2008; 2008: *Norme tecniche per le costruzioni*. Ministero delle Infrastrutture, Roma, Italy, 445 pp.

Duong K., Sheikh D. and Vecchio F.; 2007: *Seismic behavior of shear-critical reinforced concrete frame: experimental investigation*. Struct. J., **104**, 304-313.

Fajfar P. and Gašperšič P.; 1996: *The N2 method for the seismic damage analysis of R/C buildings*. Earthquake Eng. Struct. Dyn., **25**, 31-46.

Fava G., Carvelli V. and Pisani M.; 2016: *Remarks on bond of GFRP rebars and concrete*. Composites Part B, **93**, 210-220.

FEMA 356; 2000: *Prestandard and commentary for the seismic rehabilitation of buildings*. Federal Emergency Management Agency, Washington, DC, USA, 518 pp.

Fibre Net S.r.l.; 2015: <www.fibrenet.it.>.

Fragiadakis M. and Papadrakakis M.; 2008: *Performance-based optimum seismic design of reinforced concrete structures*. Earthquake Eng. Struct. Dyn., **37**, 825-844.

Ganzerli S., Pantelides C. and Reaveley L.; 2000: *Performance-based design using structural optimization*. Earthquake Eng. Struct. Dyn., **29**, 1677-1690.

Gattesco N., Amadio C. and Bedon C.; 2015: *Experimental and numerical study on the shear behavior of stone masonry walls strengthened with GFRP reinforced mortar coating and steel-cord reinforced repointing*. Eng. Struct., **90**, 143-157.

Gattulli V., Lampis G., Marcari G. and Paolone A.; 2014: *Simulations of FRP reinforcement in masonry panels and application to a historic facade*. Eng. Struct., **75**, 604-618.

Goldberg D.E.; 1989: *Genetic algorithms in search, optimization and machine learning*. Addison-Wesley Publishing Company Inc., New York, NY, USA, 432 pp.

International Federation for Structural Concrete; 2012: *Model Code 2010, Final draft, vol. 1*. Bulletin 65, Lausanne, Switzerland, 350 pp.

Lam L. and Teng J.G.; 2009: *Stress-strain model for FRP-confined concrete under cyclic axial compression*. Eng. Struct., **31**, 308-321.

Le-Trung K., Lee K., Lee J., Lee D.H. and Woo S.; 2010: *Experimental study of RC beam-column joints strengthened using CFRP composites*. Composites Part B, **41**, 76-85.

Ma C.-K., Apandi N.M., Yung S.C.S., Hau N.J., Haur L.W., Awang A.Z. and Omar W.; 2017: *Repair and rehabilitation of concrete structures using confinement: a review*. Constr. Build. Mater., **133**, 502-515.

Martinelli E., Perri F., Sguazzo C. and Faella C.; 2016: *Cyclic shear-compression tests on masonry walls strengthened with alternative configurations of CFRP strips*. Bull. Earthquake Eng., **14**, 1695-1720.

Megalooikonomou K.G., Monti G. and Santini S.; 2012: *Constitutive model for fiber-reinforced polymer- and tie-confined concrete*. ACI Struct. J., **109**, 569-578.

OpenSees; 2010: *Open System for earthquake engineering simulation*. <opensees.berkeley.edu/wiki/index.php/Main_Page>.

Parvin A., Altay S., Yalcin C. and Kaya O.; 2010: *CFRP rehabilitation of concrete frame joints with inadequate shear and anchorage details*. J. Compos. Constr., **14**, 72-82.

Paulay T. and Priestley M.J.N.; 1992: *Seismic design of reinforced concrete and masonry buildings*. Wiley & Sons Inc., New York, NY, USA, 768 pp.

Realfonzo R. and Napoli A.; 2013: *Confining concrete members with FRP systems: predictive vs. design strain models*. Compos. Struct., **104**, 304-319.

Realfonzo R., Martinelli E., Napoli A. and Nunziata B.; 2013: *Experimental investigation of the mechanical connection between FRP laminates and concrete*. Composites Part B, **45**, 341-355.

Rocca S., Galati N. and Nanni A.; 2008: *Review of design guidelines for FRP confinement of reinforced concrete columns of noncircular cross sections*. J. Compos. Constr., **12**, 88-92.

Samaan M., Mirmiran A. and Shahawy M.; 1998: *Model of concrete confined by fiber composites*. J. Struct. Eng., **124**, 1026-1031.

Santarsiero G. and Masi A.; 2015: *Seismic performance of RC beam-column joints retrofitted with steel dissipation jackets*. Eng. Struct., **85**, 95-106.

Scott M. and Fenves G.; 2006: *Plastic hinge integration methods for force-based beam-column elements*. J. Struct. Eng., **132**, 244-252.

SEAOC; 1995: *Vision 2000. Performance based seismic engineering for buildings - part 2: conceptual framework*. Structural Engineers Association of California, Sacramento, CA, USA.

Truong G., Kim J.-C. and Choi K.-K.; 2017: *Seismic performance of reinforced concrete columns retrofitted by various methods*. Eng. Struct., **134**, 217-235.

Vitiello U., Asprone D., Di Ludovico M. and Prota A.; 2017: *Life-cycle cost optimization of the seismic retrofit of existing RC structures*. Bull. Earthquake Eng., **15**, 2245-2271.

Yazdanbakhsh A., Bank L. and Chen C.; 2016: *Use of recycled FRP reinforcing bar in concrete as coarse aggregate and its impact on the mechanical properties of concrete*. Constr. Build. Mater., **121**, 278-284.

Zhu J., Wang X., Xu Z. and Weng C.; 2011: *Experimental study on seismic behavior of RC frames strengthened with CFRP sheets*. Compos. Struct., **93**, 1595-1603.

Zou X. and Chan C.; 2005: *Optimal seismic performance-based design of reinforced concrete buildings using nonlinear pushover analysis*. Eng. Struct., **27**, 1289-1302.

Zou X., Teng J., Lorenzis L.D. and Xia S.; 2007: *Optimal performance-based design of FRP jackets for seismic retrofit of reinforced concrete frames*. Composites Part B, **38**, 584-597.

Corresponding author: Corrado Chisari
Department of Civil Engineering, University of Salerno
Via Giovanni Paolo II 132, 84084 Fisciano (SA), Italy
Phone: +39 089 964342; e-mail: corrado.chisari@gmail.com